Copernicus SLSTR

Sea Surface Temperature Validation Report

Doc.No. : EUM/RSP/TEN/22/1289305
Issue : v1
Date : 8 March 2022
WBS/DBS :

EUMETSAT
Eumetsat-Allee 1, D-64295 Darmstadt, Germany
Tel: +49 6151 807-7
Fax: +49 6151 807 555
http://www.eumetsat.int

1 EXECUTIVE SUMMARY

This report summarises validation of Sea Surface Temperature (SST) products from the Copernicus Sea and Land Surface Temperature Radiometer (SLSTR) Baseline Collection 3 SST dataset. The following conclusions are drawn from the results presented in this report:

- SLSTR provides high-quality dual-view SSTs for use as a reference sensor
- SLSTR-A and SLSTR-B SSTs generally meet mission requirements for accuracy
  - N2 out of specification for total column water vapour loadings above 35 kg/m^2
  - New SST coefficients are being evaluated to address this limitation
- SLSTR-B is currently using the same retrieval coefficients as SLSTR-B
  - SLSTR-B is harmonised to SLSTR-A via the Sensor Specific Error Statistics (SSES) included in the SL_2_WST product

Users are reminded:

- That SLSTR provides a measure of SST_{skin}
  - Confirmed through independent validation using in situ data over multiple depths
- The SL_2_WST (Group for High Resolution SST, GHRSST, L2P format) product contains both dual-view (D2, D3) and nadir-only (N2, N3) retrievals
- To use only dual-view for reference sensor
- To use only QL=5 data
  - Never use D2 or D3 QL=4 data
- To **always** apply the SSES_bias adjustments
- To please read the Product Notices as they provide a lot of useful information

Table of Contents

1 INTRODUCTION

This report presents an assessment of Sea Surface Temperature (SST) data quality of Baseline Collection 3 of the Copernicus Sea and Land Surface Temperature Radiometer (SLTSR, RD-1) dataset, comprising data from SLSTR-A launched on Sentinel3-A on 16th February 2016, and SLSTR-B launched on Sentinel-3B on 25th April 2018. SST products started to be delivered operationally from the European Organisation for the Exploitation of Meteorological Satellites (EUMETSAT) marine centre on 5th July 2017 and 12th March 2019 respectively.

The SLSTR Baseline Collection 3 SST dataset comprises data produced operationally by EUMETSAT in either Near-Real Time (NRT) or Non Time Critical (NTC) mode as well as data reprocessed offline. The SLSTR Baseline Collection number is included in the Standard Archive Format for Europe (SAFE) format filename. Reprocessed NTC products are distinguished from operational NTC products by the letter R instead of the letter O in the platform field in the SLSTR SAFE format filename. Users are referred to the most recent SLSTR Level 2 Marine Product Notice available from http://slstr.eumetsat.int for details on how to assemble a consistent Baseline Collection 3 SST dataset.

The mission requirements for SST from SLSTR is a target of 0.3 K with a temporal stability better than 0.1 K / decade [RD-2; RD-3]. The assessment of data quality against these requirements is summarised in the Sentinel 3 Calibration and Validation Plan [RD-4]. The main aim of this document is to summarise comparisons to validation data taken *in situ* or from ships of opportunity and research vessels.

There are two different SST products that require validation. These are:

- SL_2_WCT
  These products contain all possible SSTs generated per pixel and provided in a SAFE set of files. These products are internal products available to validation users.

- SL_2_WST
  These products contain the best SST per-pixel provided in an Group for High Resolution SST (GHRSST) L2P format file.

The SLSTR instruments have three spectral bands that are used for SST retrieval, with nominal band centres at 3.7 µm (S7), 11 µm (S8) and 12 µm (S9). During the day the 3.7 µm channel is not used due to solar contamination and so, as each Earth scene is viewed in both nadir and off-nadir, there are four possible retrieved SSTs, referred to as N2 (nadir-only 11 µm and 12 µm), N3 (nadir-only 3.7 µm, 11 µm and 12 µm), D2 (dual-view 11 µm and 12 µm) and D3 (dual-view 3.7 µm, 11 µm and 12 µm). The N2, N3, D2 and D3 nomenclature is used through the rest of this report and all four retrievals are provided in the SL_2_WCT product.

The SL_2_WST product contains the best SST available, which due to the different size of the nadir and oblique grids means the product contains a mixture of dual-view and nadir-only retrievals. Flags in the product can be used to identify which retrieval type is used per pixel. For dual-view retrievals the equivalent nadir-only SST can be calculated by applying the dual minus nadir SST difference field applied in the product per pixel.

The retrieval scheme itself uses linear regression algorithms with coefficients derived from radiative transfer models that perform a linear regression of SST to simulated brightness temperatures (BTs) at the nominal band centres. The physical basis and forward modelling used within the ATSR Reprocessing for Climate (ARC) project [RD-5] has been applied to SLSTR. Cloud identification uses a method of clear-sky identification resulting from applying Bayes theorem to simulated clear-sky BTs output from a radiative transfer model [RD-6].

2 REFERENCE DATA

The primary reference dataset for SST_{skin} measurements provided by infrared (IR) satellite instruments such as the SLSTRs are ship-borne radiometers, which also have the advantage of being completely traceable to agreed SI standards through national metrology institutes. However, the coverage and availability of ship-borne radiometric data is not ideal, which limits any long-term drift assessment and does not allow for a global assessment of the SST_{skin} data quality. Other potential reference data include surface drifting buoys, Argo floats, moored buoys, and conventional ship measurements from engine room intakes or hull-mounted sensors.

Although the uncertainty of the non-radiometer datasets is not always fully-traceable to an SI temperature standard, they are important datasets for satellite SST validation due to their significantly improved global coverage compared to other potential reference datasets, particularly for drifting buoys. In addition, these other datasets provide SST at depth and require adjustment to skin to be used correctly for SST validation. However, under certain conditions (wind speed > 6 ms^{-1}) a constant offset of around -0.17 K is expected [RD-7].

A summary of all validation data used in the analysis presented in this report is given in Table 2-1.

Data type	Time period	Coverage	Depth
Shipborne IR radiometers	2016 – 2018	Various single cruise tracks	SST_{skin}
Argo floats	2016 – 2022	Global	SST_{depth}
Moorings	2016 – 2022	Coastal and Tropics	SST_{depth}
Drifting buoys	2016 - 2022	Global	SST_{depth}

Table 2-1: *Content of validation dataset*

All available ship-borne radiometer data were acquired from the instrument Principle Investigators (PI) through the International Sea Surface Temperature (SST) Fiducial Reference Measurement (FRM) Radiometer Network (ISFRN, https://ships4sst.org/), No additional quality control (QC) was applied to the radiometer data at this point. Drifting buoy, moored buoy and Argo data are provided by the Copernicus Marine Environment Service (CMEMS) in situ Thematic Assembly Centre (TAC). All data are subject to basic QC by CMEMS and no further QC was done. For Argo, the nearest to the surface measurement passing the CMEMS quality tests between 3.5 m and 5.5 m in depth was used.

To compare the SLSTR SSTs to in situ measurements across different depths (e.g. to drifting buoys at a depth of 20 cm) the in situ SSTs are adjusted to SSTskin. A second adjustment is made to minimise the difference between the in situ and satellite measurement times. To model both of these adjustments we calculate two differential temperatures using a combined skin and diurnal variability model (Fairall et al.,/Kantha and Clayson, FKC, [RD-8,RD-9]) as demonstrated in Embury et al. [RD-10]. The current implementation of the FKC model was developed at the Met Office (Horrocks et al., [RD-11]) with settings given in Embury et al. [RD-10]. The model is driven by fluxes from ECMWF model fields from the ERA-5 reanalysis [RD-12].

3 METHODOLOGY

Match-ups between SLSTR and the various validation data were found using Felyx [RD-13] to the nearest SLSTR pixel within ± 2 hours of the satellite overpass for drifters and ± 6 hours for all other in situ types, and stored within a match-up dataset (MD) for subsequent statistical and graphical analysis. The same analysis software was used to match SLSTR to all validation data in order to remove the possibility of errors due to inconsistent analysis.

Although the reference data have been subject to some basic quality control (QC) by the data provider, instances of poor data quality can cause outliers in any subsequent validation analysis. Outliers can also be due to the spatial and temporal miss-match, and of course issues with SLSTR data quality. To deal with a small number of expected outliers, robust statistics are used in the analysis.

Discrepancies and robust standard deviations are calculated for each type of validation data. Time series of discrepancy and robust standard deviation are provided, as well as the dependence of key instrument and retrieval parameters. Spatial variations are also presented.

4 RESULTS

The following section contains the detailed validation results for the SLSTR Baseline Collection 3 SL_2_WCT and SL_2_WST products for SLSTR-A and SLSTR-B. The results include:

- Match-ups to four different reference datasets
    - Drifting buoys providing SST_{depth} adjusted to SSTskin
    - Argo floats providing SST_{depth} adjusted to SSTskin
    - Coastal and tropical moorings providing SST_{depth} adjusted to SSTskin
    - Ship-borne radiometers providing SST_{skin}
- Adjustments have been made to make the reference dataset equivalent to SST_{skin} at the time of the satellite overpass using the FKC model as described earlier.
- Dependence plots of median and robust standard deviation of the discrepancy between the satellite SST_{skin} versus reference SST_{skin}.
- Results are shown for data with a quality level of 5 only and the SSES_bias field has been applied. These fields are calculated offline for the SL_2_WCT product.
    - For both NR and L2P match-ups, dependences are provided for (top row, left to right) latitude, time difference between satellite and drifter measurements, year, (bottom row, left to right) wind speed, solar zenith angle and across-track position. Different channel combinations are shown by the indicated colours, with dual-view results represented as sold lines and nadir-only results as dashed lines.
    - Ideally the plots will show a zero bias, with no dependence on the variable on the abscissa, and a robust standard deviation less than 0.3 K.
- Spatial maps of the median discrepancy between the satellite and the reference datasets. The greyed region indicates a band of +/- 0.1 K around zero difference.
    - Maps are shown for (top row, left to right) N2 daytime, N2 nighttime, N3 nighttime, (bottom row, left to right) D2 daytime, D2 nighttime and D3 nighttime.
    - Ideally the plots will show no spatial variability with differences less than 0.1 K (i.e. within the grey region on the colourbar).
- A summary table showing the median discrepancy and robust standard deviation of the complete set of match-ups to each available validation dataset.

4.1 SLSTR-A SL_2_WCT results

4.1.1 Comparisons between SLSTR-A WCT SSTs and drifting buoys

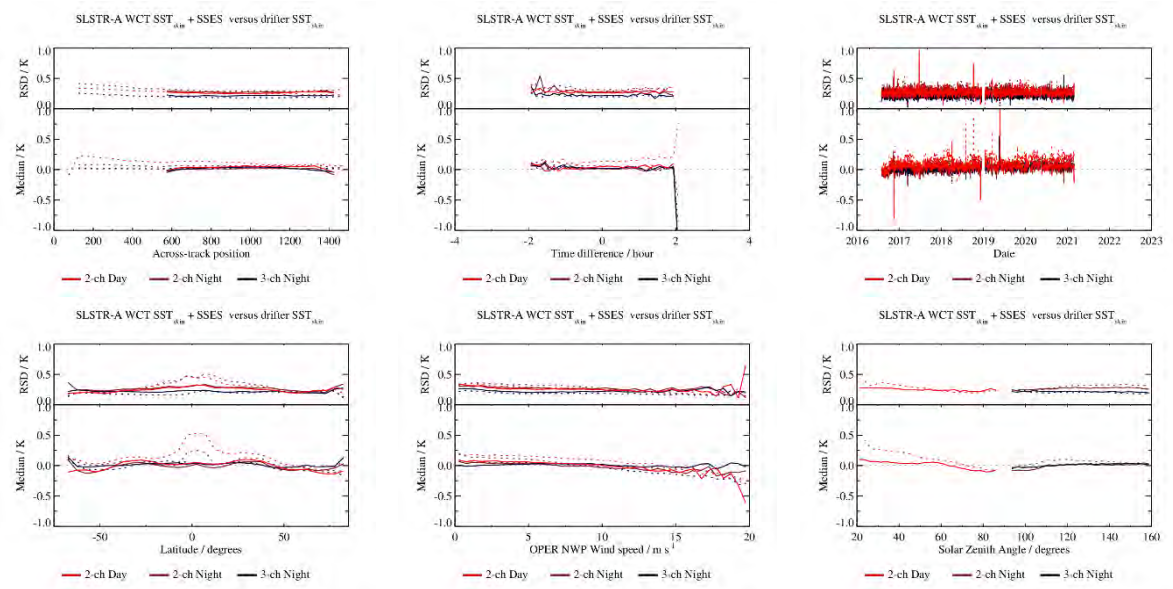

Figure 4-1: *Dependence of the median and robust standard deviation between SLSTR-A WCT SST_{skin} and drifter SST_{skin}.*

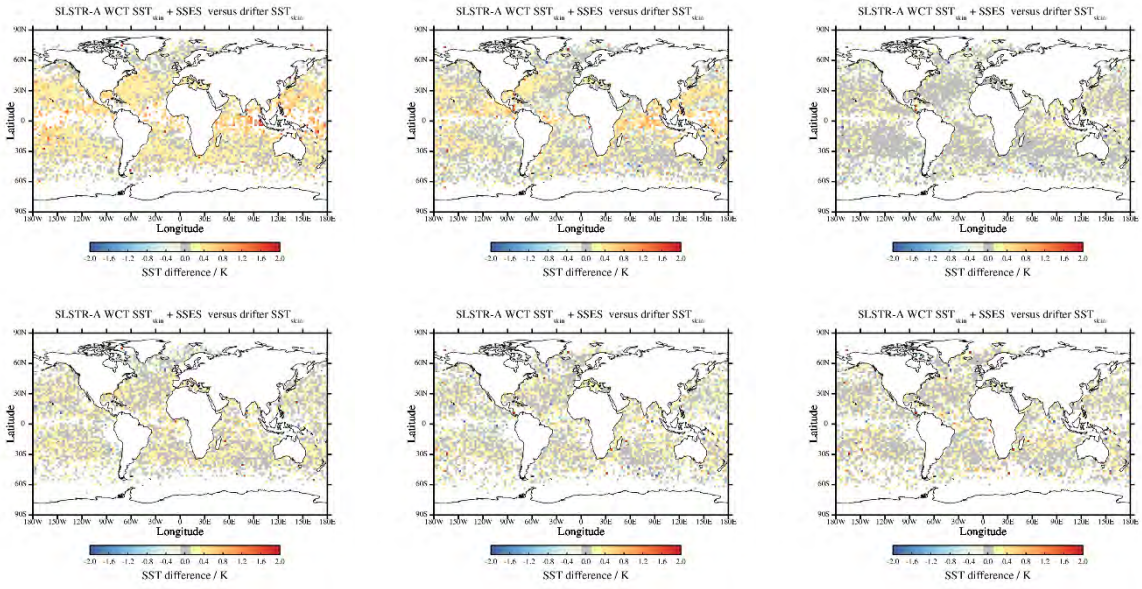

Figure 4-2: *Spatial distribution of the median discrepancy between SLSTR-A WCT SST_{skin} and drifter SST_{skin}.*

4.1.2 Comparisons between SLSTR-A WCT SSTs and Argo

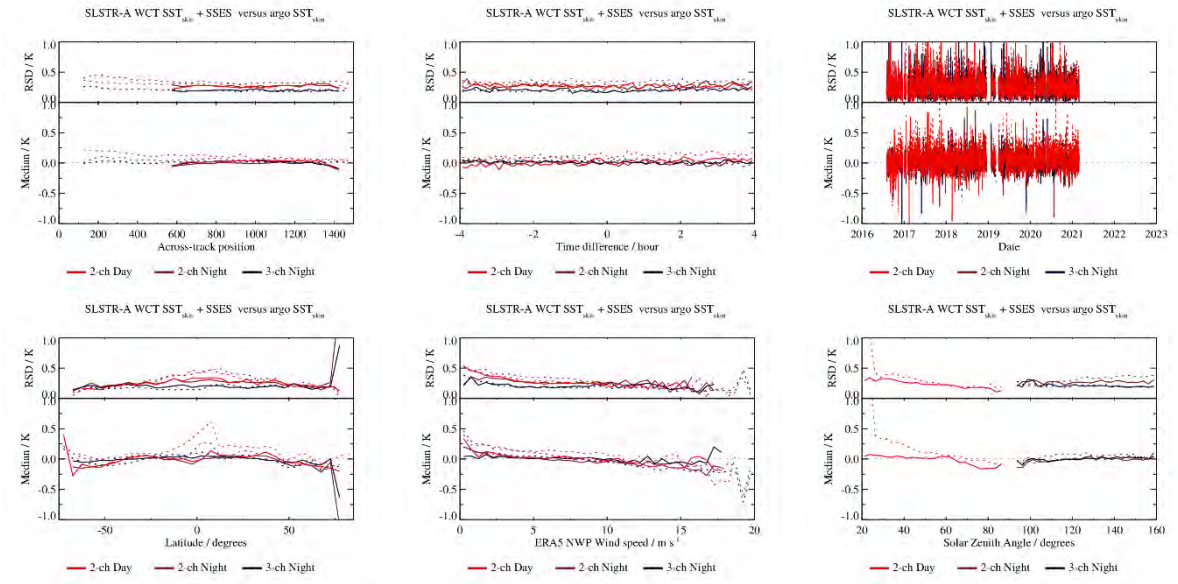

Figure 4-3: *Dependence of the median and robust standard deviation between SLSTR-A WCT SST_{skin} and Argo SST_{skin}.*

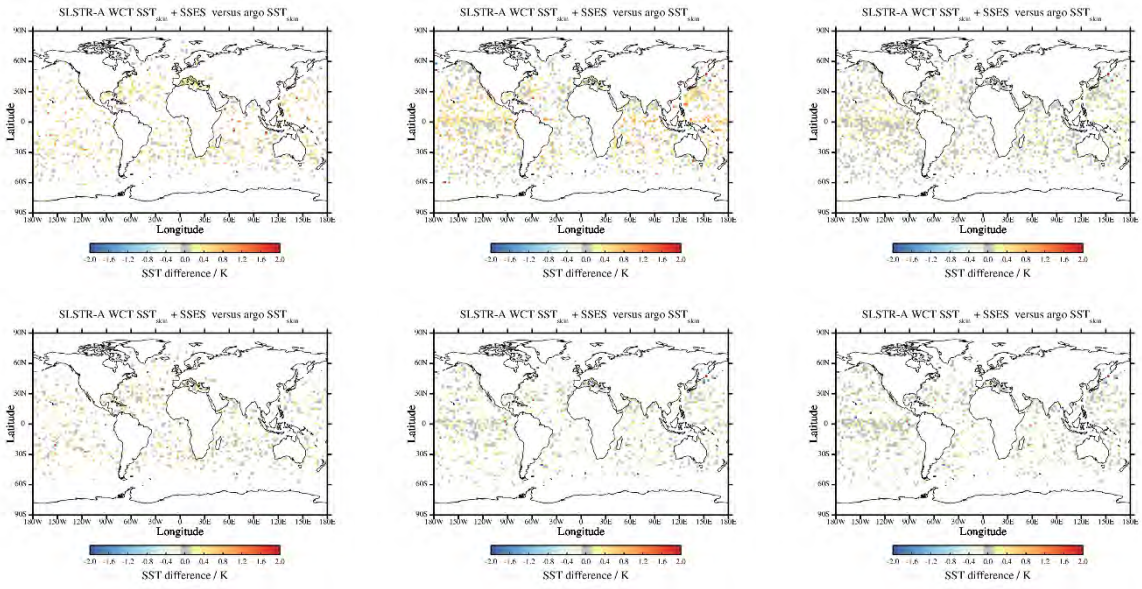

Figure 4-4: *Spatial distribution of the median discrepancy between SLSTR-A WCT SST_{skin} and Argo SST_{skin}.*

4.1.3 Comparisons between SLSTR-A WCT SSTs and moorings

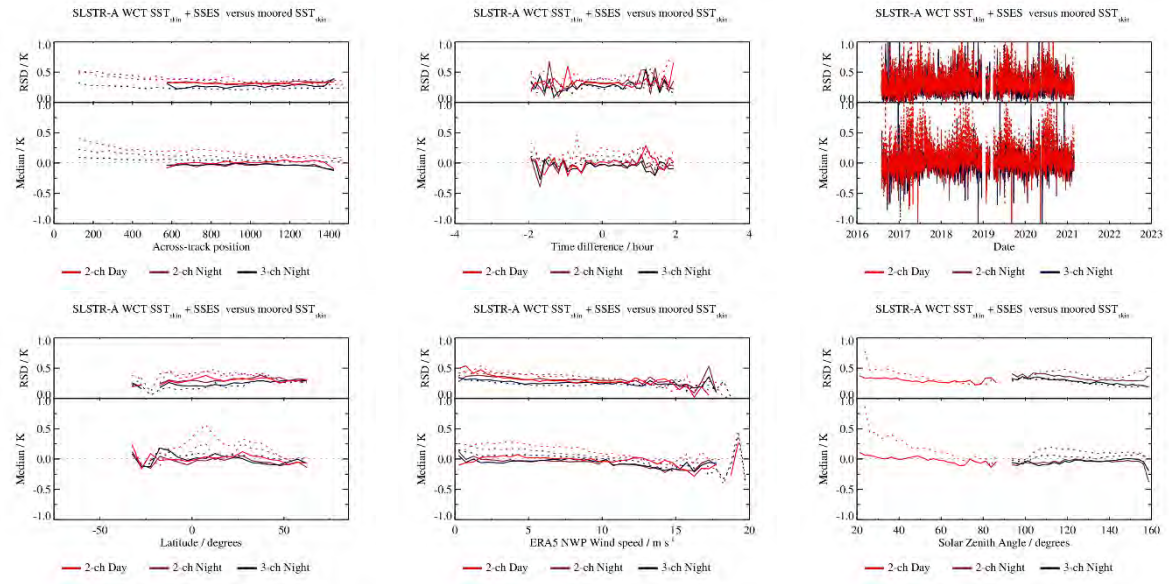

Figure 4-5: *Dependence of the median and robust standard deviation between SLSTR-A WCT SST_{skin} and mooring SST_{skin}.*

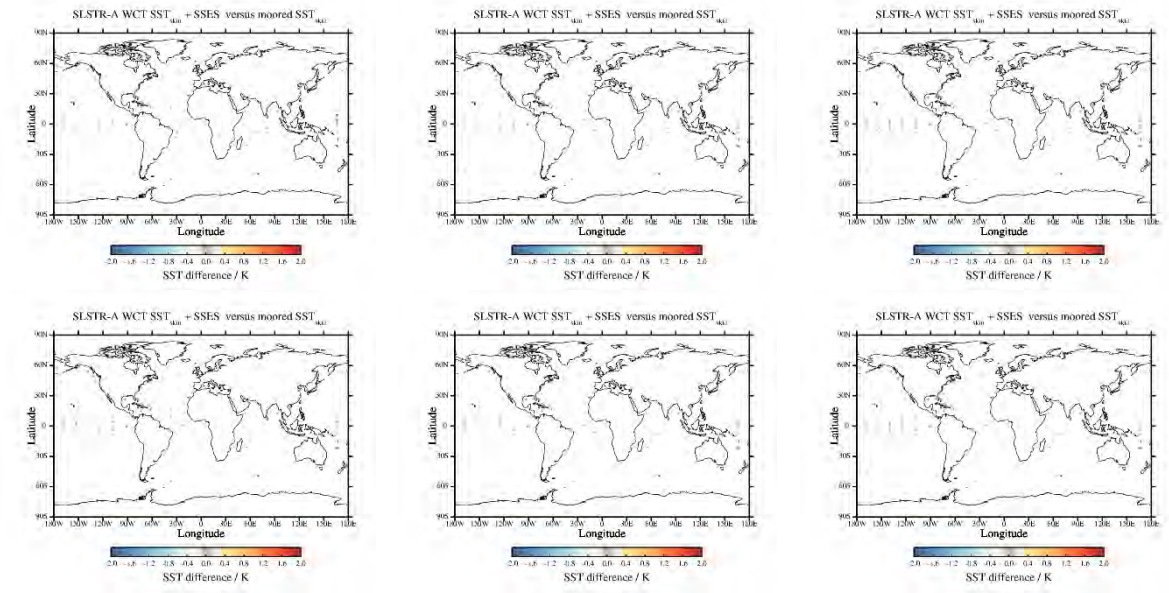

Figure 4-6: *Spatial distribution of the median discrepancy between SLSTR-A WCT SST_{skin} and mooring SST_{skin}.*

4.1.4 Comparisons between SLSTR-A WCT SSTs and radiometers

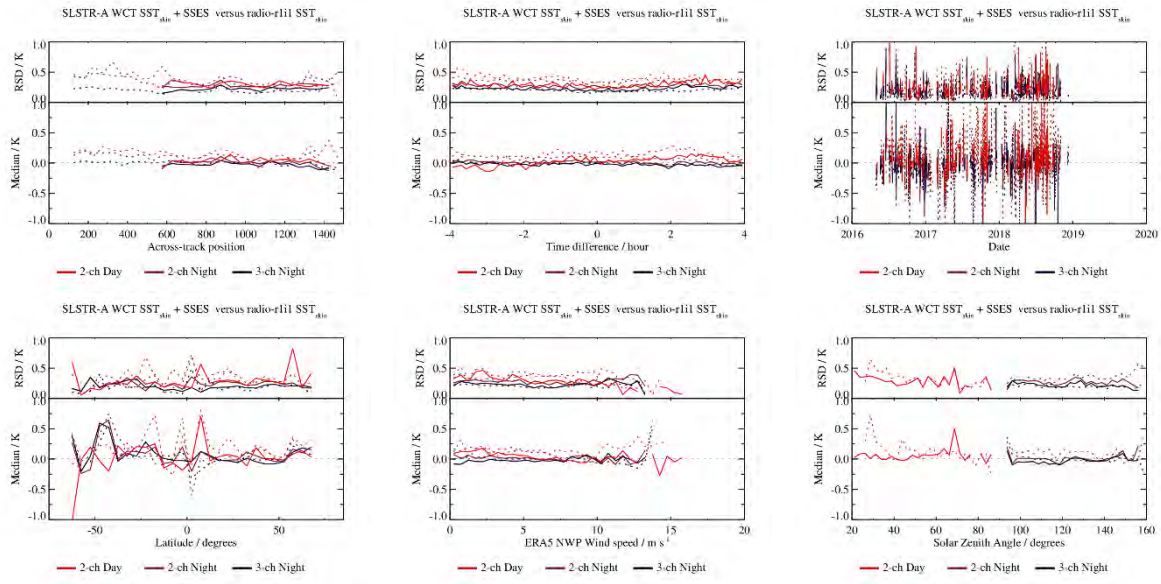

Figure 4-7: *Dependence of the median and robust standard deviation between SLSTR-A WCT SST_{skin} and radiometer SST_{skin}.*

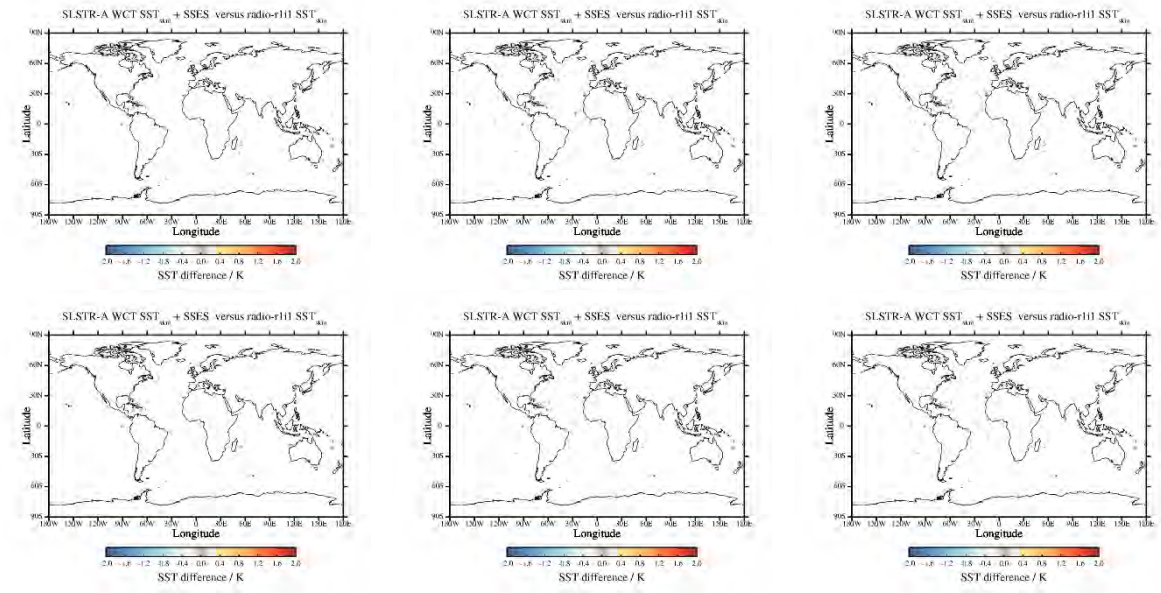

Figure 4-8: *Spatial distribution of the median discrepancy between SLSTR-A WCT SST_{skin} and radiometer SST_{skin}.*

4.1.5 Statistical analysis of SLSTR-A WCT SST validation results

Reference	Retrieval	Number	Median (K)	RSD (K)
Drifters	*Day N2*	120846	+0.13	0.29
	Day D2	117907	+0.04	0.26
	Night N2	202006	+0.06	0.31
	Night N3	202025	+0.02	0.20
	Night D2	100914	+0.01	0.28
	Night D3	100905	+0.02	0.22
Mooring	*Day N2*	17631	+0.21	0.39
	Day D2	19235	+0.01	0.31
	Night N2	30905	+0.11	0.39
	Night N3	30903	+0.04	0.24
	Night D2	16973	-0.04	0.32
	Night D3	16970	-0.03	0.27
Argo	*Day N2*	9776	+0.13	0.30
	Day D2	560	+0.02	0.27
	Night N2	20324	+0.06	0.34
	Night N3	20325	+0.02	0.20
	Night D2	10454	-0.01	0.27
	Night D3	10454	+0.01	0.20
Radiometers	*Day N2*	6973	+0.14	0.39
	Day D2	7367	+0.04	0.30
	Night N2	24767	+0.10	0.36
	Night N3	24767	-0.01	0.20
	Night D2	13730	+0.01	0.28
	Night D3	13730	-0.02	0.22

Table 4-1: *Global validation statistics from comparing SLSTR-A Baseline Collection 3 WCT SSTs to the available validation datasets.*

4.1.6 Discussion

The results show SLSTR-A WCT SSTs are generally meeting the mission requirements. No clear dependence is seen aside from the N2 retrieval, which has a warm bias and shows a strong dependency on TCWV above 35 Kg m^{-2}. The warm bias in the N2 retrieval is also seen in the spatial maps. A large proportion of the nighttime spatial maps for the other retrievals show results in the +/1 0.1 K range. Some cool biases are seen in the regions of desert dust for both N2 and N3. A high degree of consistency is seen between results from the different reference datasets.

4.2 SLSTR-A SL_2_WST results

4.2.1 Comparisons between SLSTR-A WST SSTs and drifting buoys

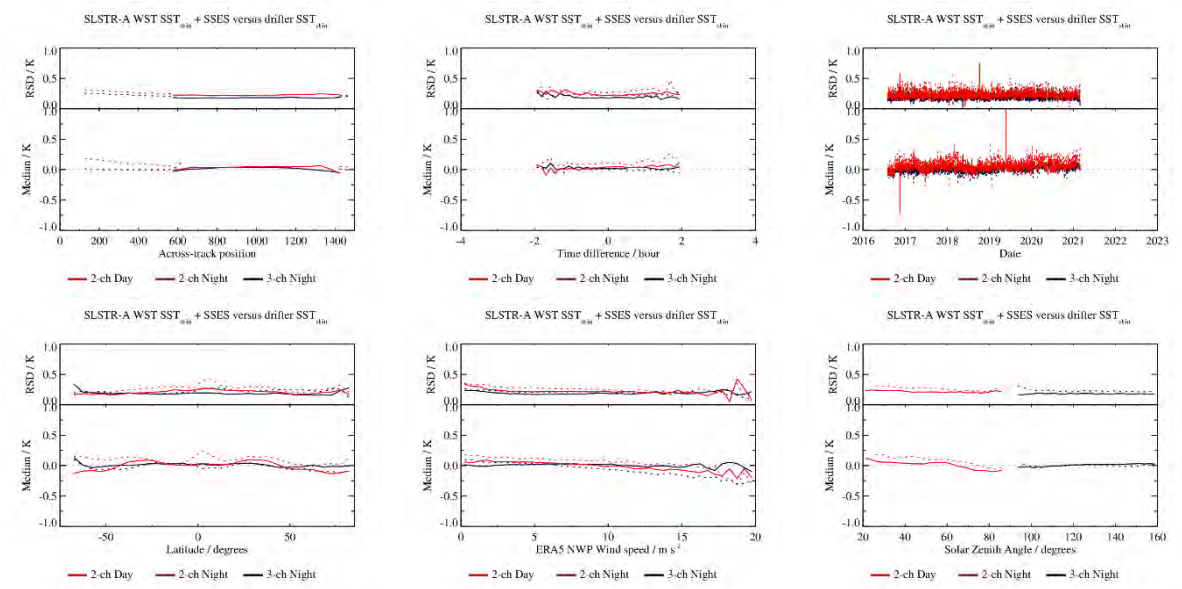

Figure 4-9: *Dependence of the median and robust standard deviation between SLSTR-A WST SST_{skin} and drifter SST_{skin}.*

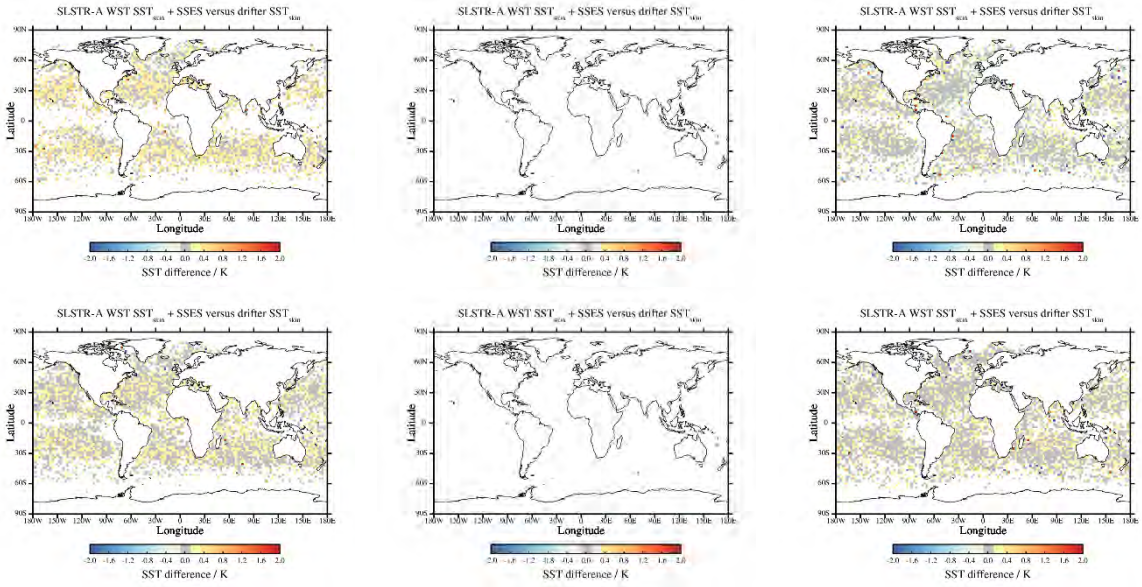

Figure 4-10: *Spatial distribution of the median discrepancy between SLSTR-A WST SST_{skin} and drifter SST_{skin}.*

4.2.2 Comparisons between SLSTR-A WST SSTs and Argo

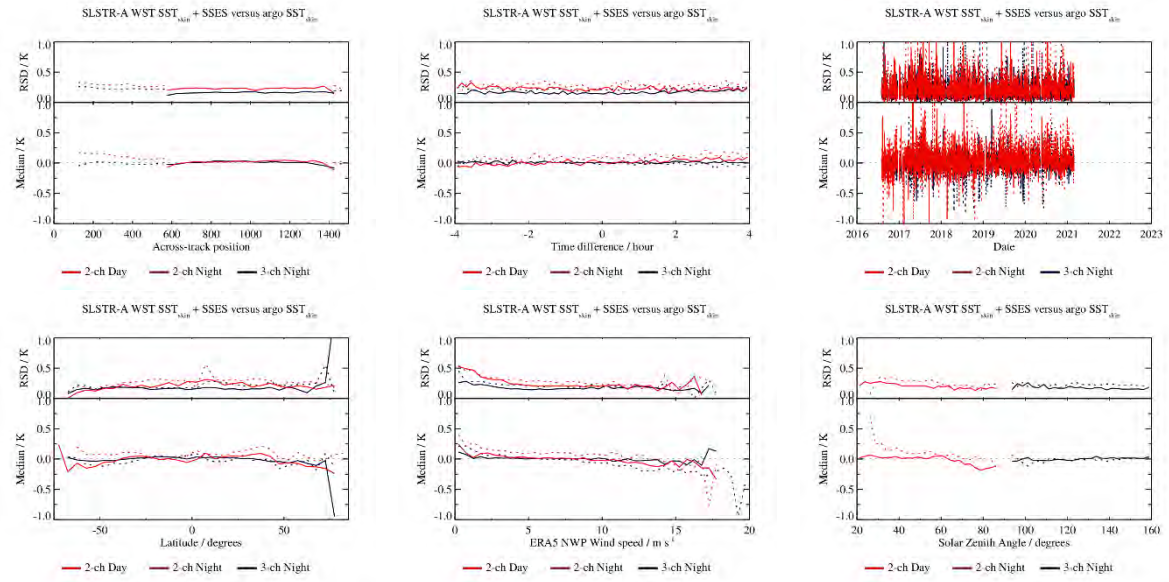

Figure 4-11: *Dependence of the median and robust standard deviation between SLSTR-A WST SST_{skin} and Argo SST_{skin}.*

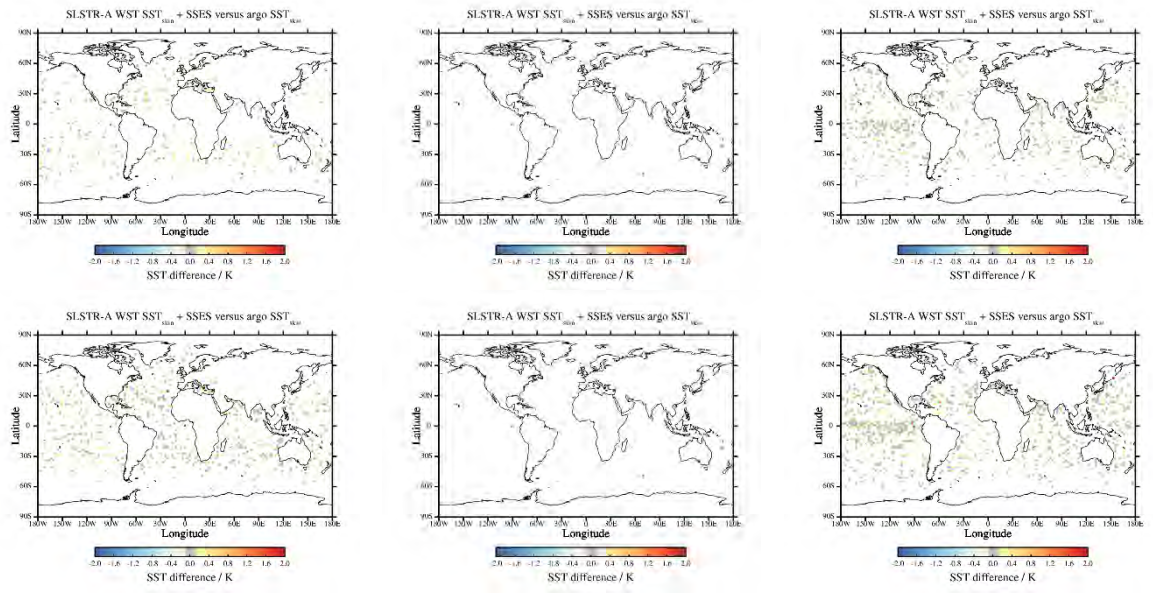

Figure 4-12: *Spatial distribution of the median discrepancy between SLSTR-A WST SST_{skin} and Argo SST_{skin}.*

4.2.3 Comparisons between SLSTR-A WST SSTs and moorings

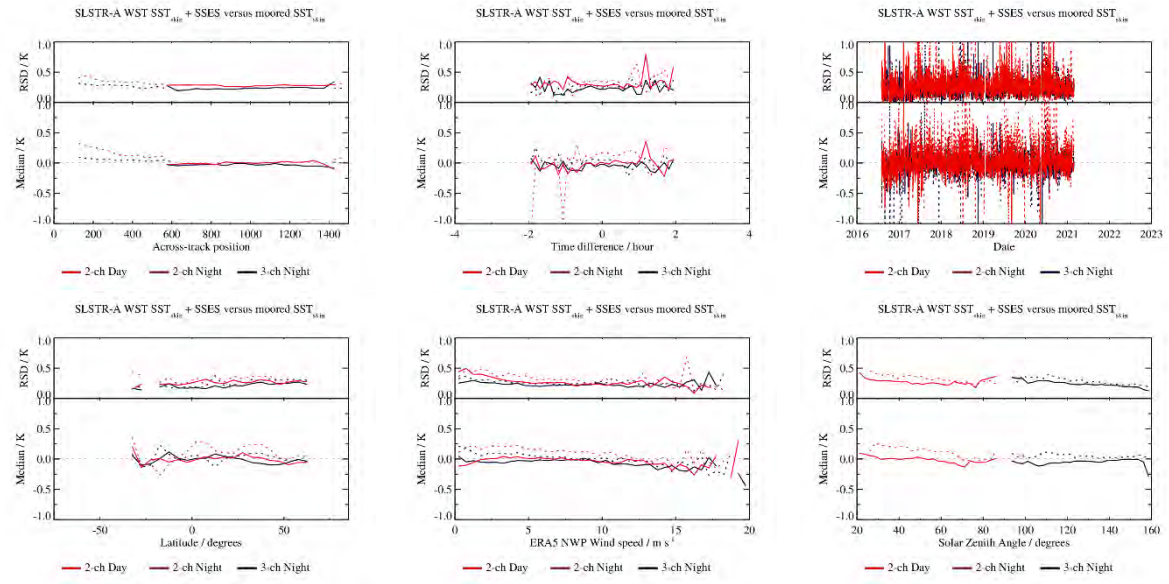

Figure 4-13: *Dependence of the median and robust standard deviation between SLSTR-A WST SST_{skin} and mooring SST_{skin}.*

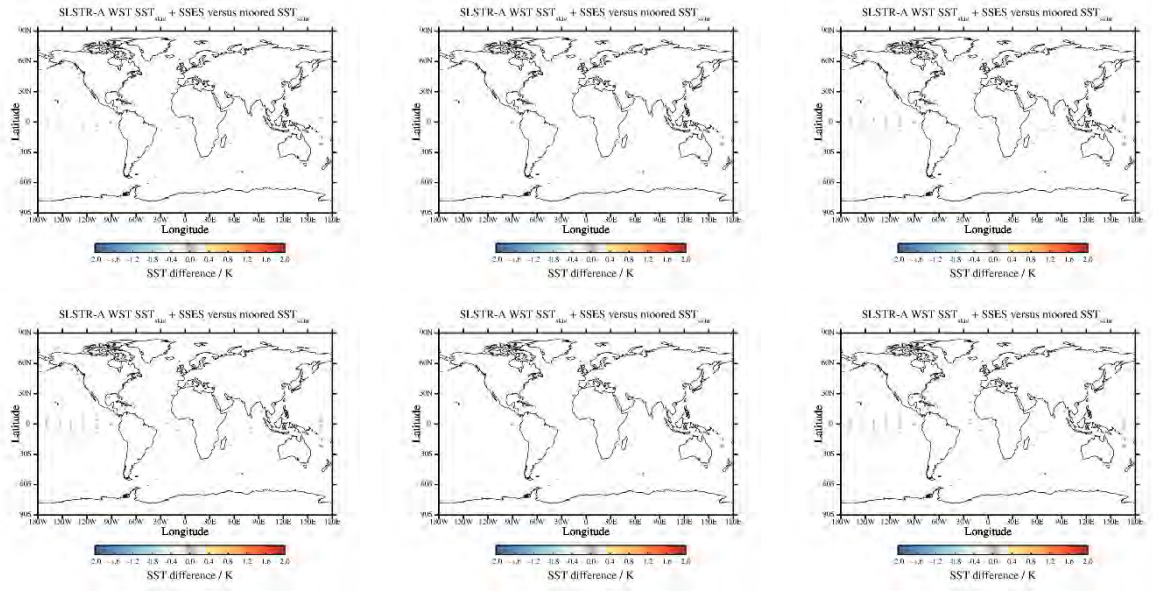

Figure 4-14: *Spatial distribution of the median discrepancy between SLSTR-A WCST SST_{skin} and mooring SST_{skin}.*

4.2.4 Comparisons between SLSTR-A WST SSTs and radiometers

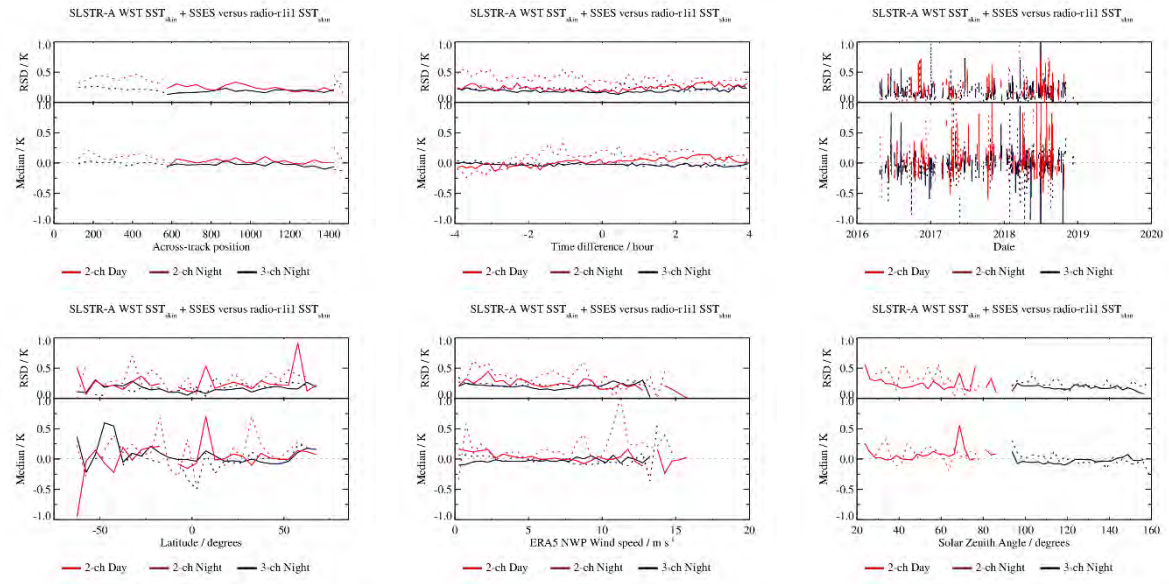

Figure 4-15: *Dependence of the median and robust standard deviation between SLSTR-A WST SST_{skin} and radiometer SST_{skin}.*

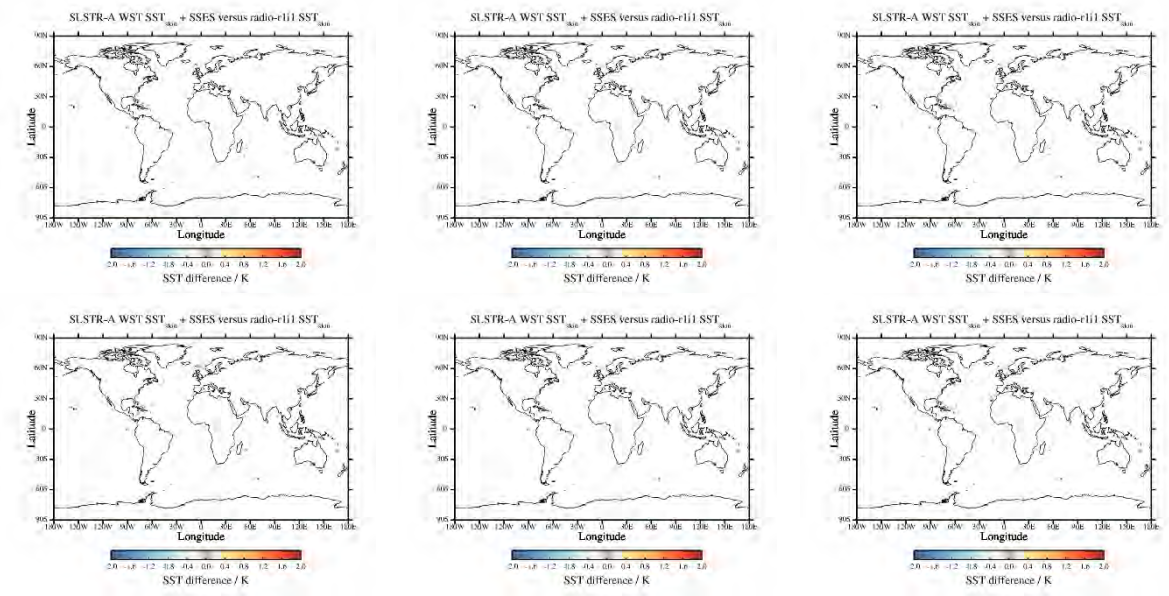

Figure 4-16: *Spatial distribution of the median discrepancy between SLSTR-A WST SST_{skin} and radiometer SST_{skin}.*

4.2.5 Statistical analysis of SLSTR-A WST SST validation results

Reference	Retrieval	Number	Median (K)	RSD (K)
Drifters	*Day N2*	54110	+0.10	0.28
	Day D2	105886	+0.04	0.22
	Night N3	78683	+0.01	0.22
	Night D3	103843	+0.02	0.18
Mooring	*Day N2*	7937	+0.15	0.35
	Day D2	18286	-0.01	0.28
	Night N3	12037	+0.04	0.26
	Night D3	17527	-0.03	0.23
Argo	*Day N2*	4601	+0.10	0.29
	Day D2	8633	+0.02	0.23
	Night N3	7923	-0.01	0.22
	Night D3	10763	+0.01	0.16
Radiometers	*Day N2*	3189	+0.10	0.40
	Day D2	6350	+0.03	0.25
	Night N3	9045	-0.02	0.23
	Night D3	14022	-0.03	0.19

Table 4-2: *Global validation statistics from comparing SLSTR-A Baseline Collection 3 WST SSTs to the available validation datasets.*

4.2.6 Discussion

The results show similar findings to the SLSTR-A WCT results. In general the biases are slightly cooler and also have smaller robust standard deviations. This is due to the atmospheric smoothing applied to the L2P SSTs, which reduces atmospheric noise on the retrieval. However, a small amount of residual cloud contamination will also then be smoothed with the SSTs.

4.3 SLSTR-B SL_2_WCT results

4.3.1 Comparisons between SLSTR-B WCT SSTs and drifting buoys

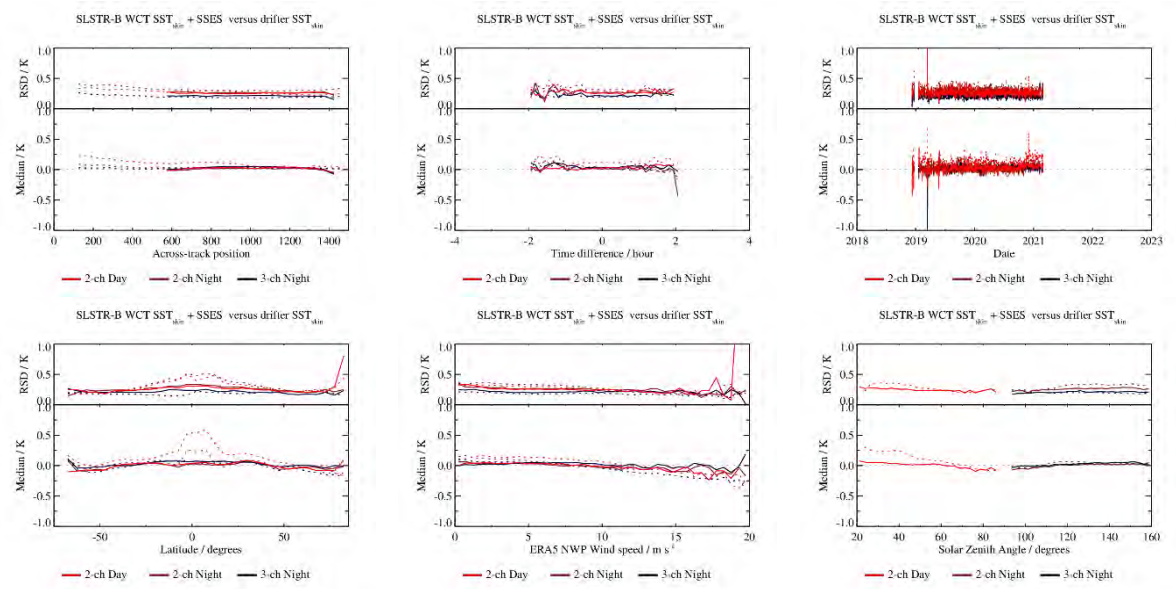

Figure 4-17: *Dependence of the median and robust standard deviation between SLSTR-B WCT SST_{skin} and drifter SST_{skin}.*

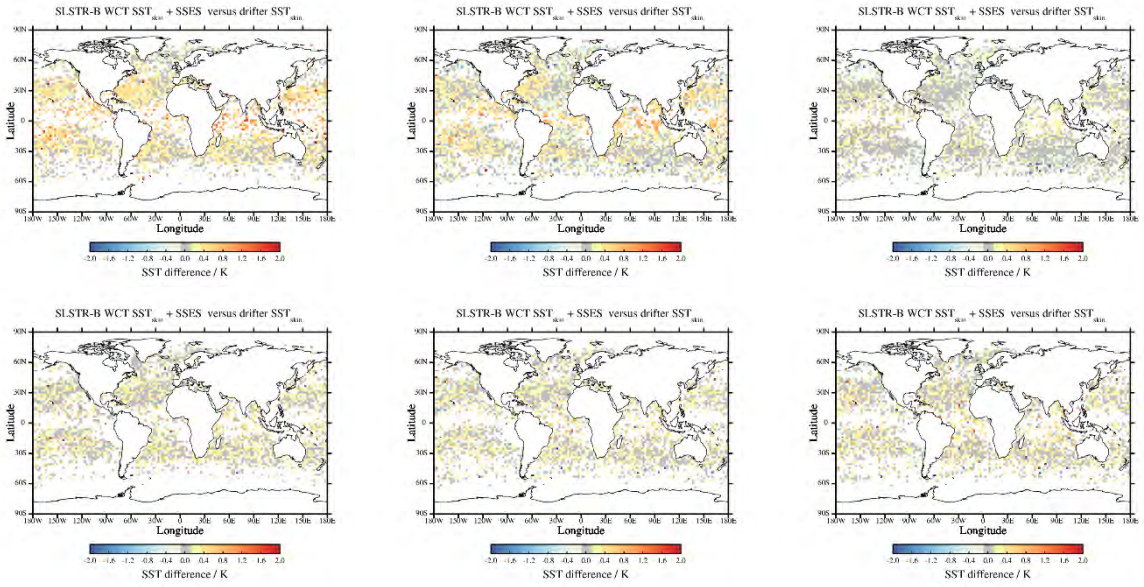

Figure 4-18: *Spatial distribution of the median discrepancy between SLSTR-B WCT SST_{skin} and drifter SST_{skin}.*

4.3.2 Comparisons between SLSTR-B WCT SSTs and Argo

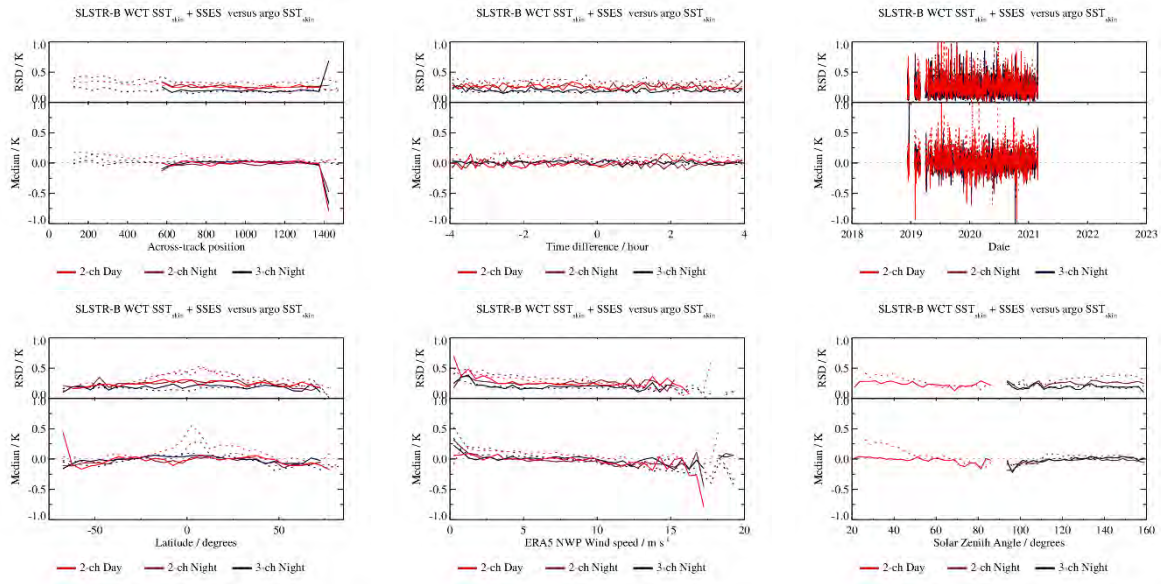

Figure 4-19: *Dependence of the median and robust standard deviation between SLSTR-B WCT SST_{skin} and Argo SST_{skin}.*

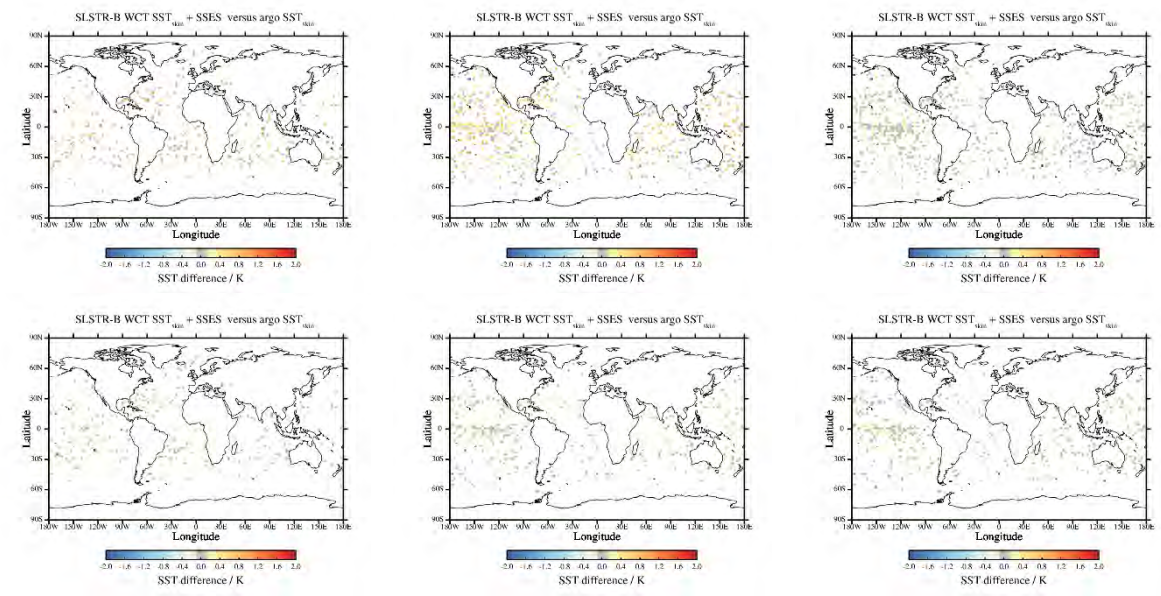

Figure 4-20: *Spatial distribution of the median discrepancy between SLSTR-B WCT SST_{skin} and Argo SST_{skin}.*

4.3.3 Comparisons between SLSTR-B WCT SSTs and moorings

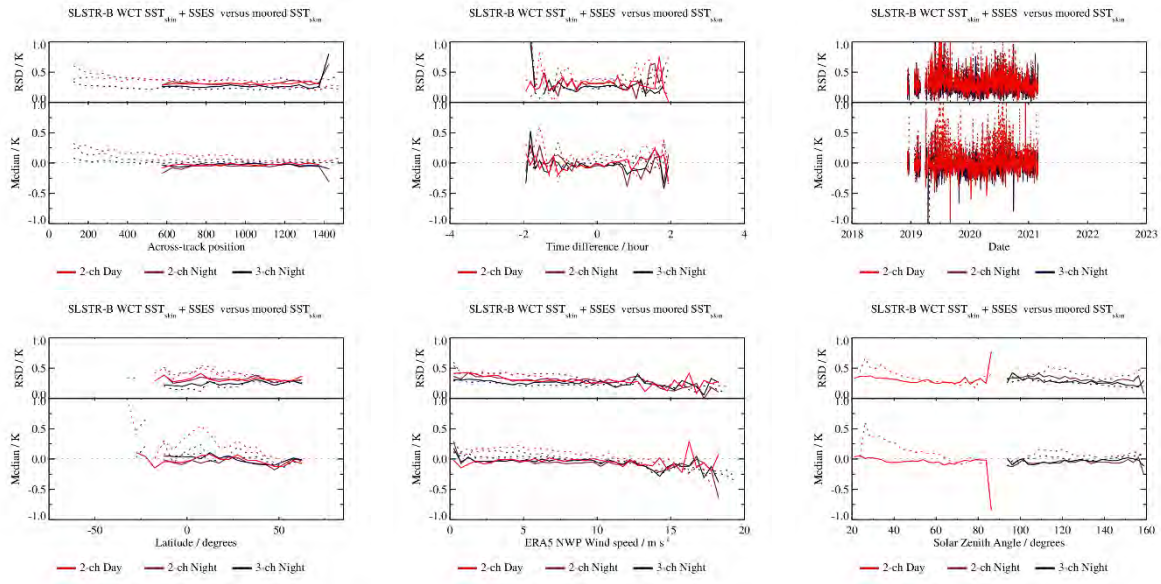

Figure 4-21: *Dependence of the median and robust standard deviation between SLSTR-B WCT SST_{skin} and mooring SST_{skin}.*

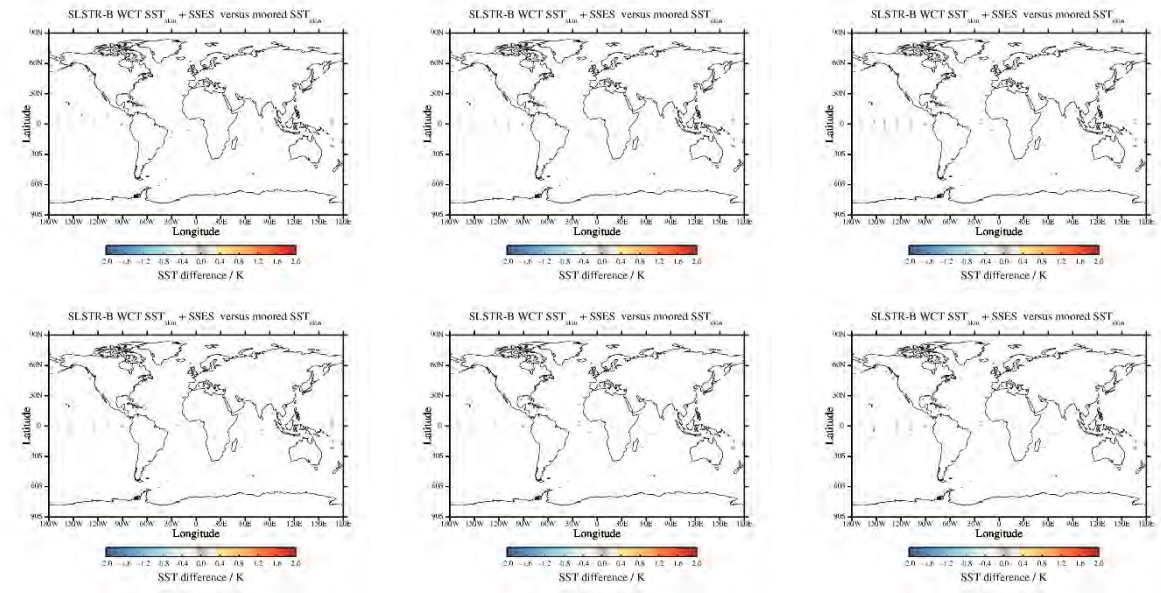

Figure 4-22: *Spatial distribution of the median discrepancy between SLSTR-B WCT SST_{skin} and mooring SST_{skin}.*

4.3.4 Statistical analysis of SLSTR-B WCT SST validation results

Reference	Retrieval	Number	Median (K)	RSD (K)
Drifters	*Day N2*	59985	+0.11	0.30
	Day D2	57494	+0.03	0.26
	Night N2	99171	+0.04	0.32
	Night N3	99168	+0.02	0.20
	Night D2	48542	+0.01	0.27
	Night D3	48541	+0.03	0.21
Mooring	*Day N2*	9817	+0.14	0.36
	Day D2	9917	-0.03	0.31
	Night N2	16120	+0.06	0.39
	Night N3	16120	+0.01	0.24
	Night D2	8554	-0.06	0.32
	Night D3	8554	-0.03	0.26
Argo	*Day N2*	4832	+0.10	0.30
	Day D2	4618	+0.01	0.26
	Night N2	9583	+0.04	0.35
	Night N3	9583	+0.01	0.19
	Night D2	4767	-0.02	0.26
	Night D3	4769	+0.01	0.19

Table 4-3: *Global validation statistics from comparing SLSTR-B Baseline Collection 3 WCT SSTs to the available validation datasets.*

4.3.5 Discussion

The results for SLSTR-B WCT are in good agreement with those for SLSTR-A. All retrievals are within requirements aside from the N2 retrieval at TCWV loadings above 35 Kg m^{-2}. The SLSTR-B SST retrieval currently uses SLSTR-B coefficients and are harmonised via the SSES_bias term.

4.4 SLSTR-B SL_2_WST results

4.4.1 Comparisons between SLSTR-B WST SSTs and drifting buoys

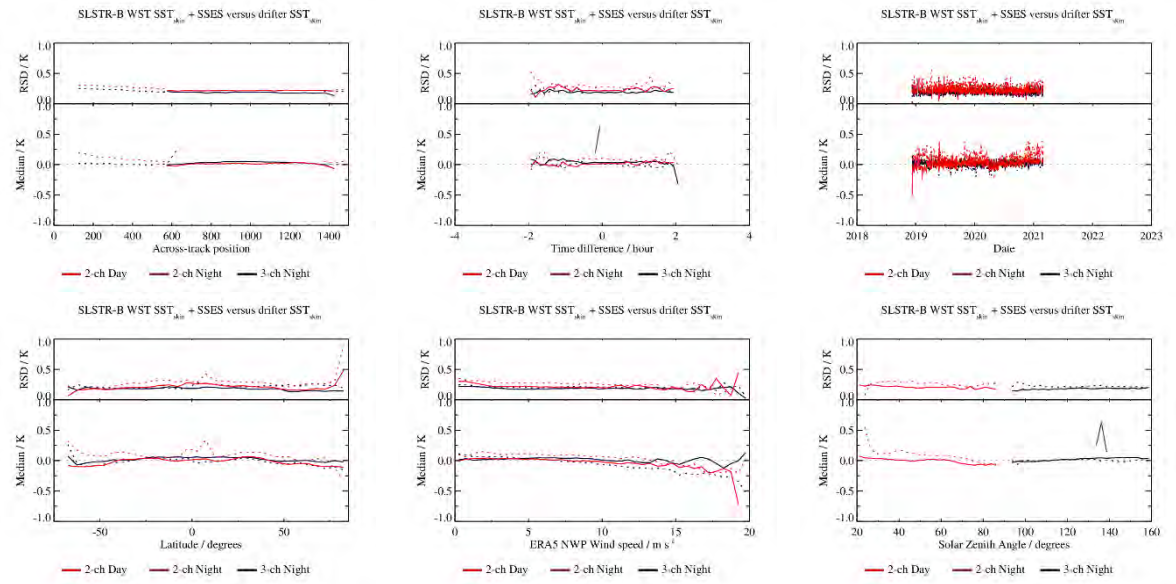

Figure 4-23: *Dependence of the median and robust standard deviation between SLSTR-B WST SST_{skin} and drifter SST_{skin}.*

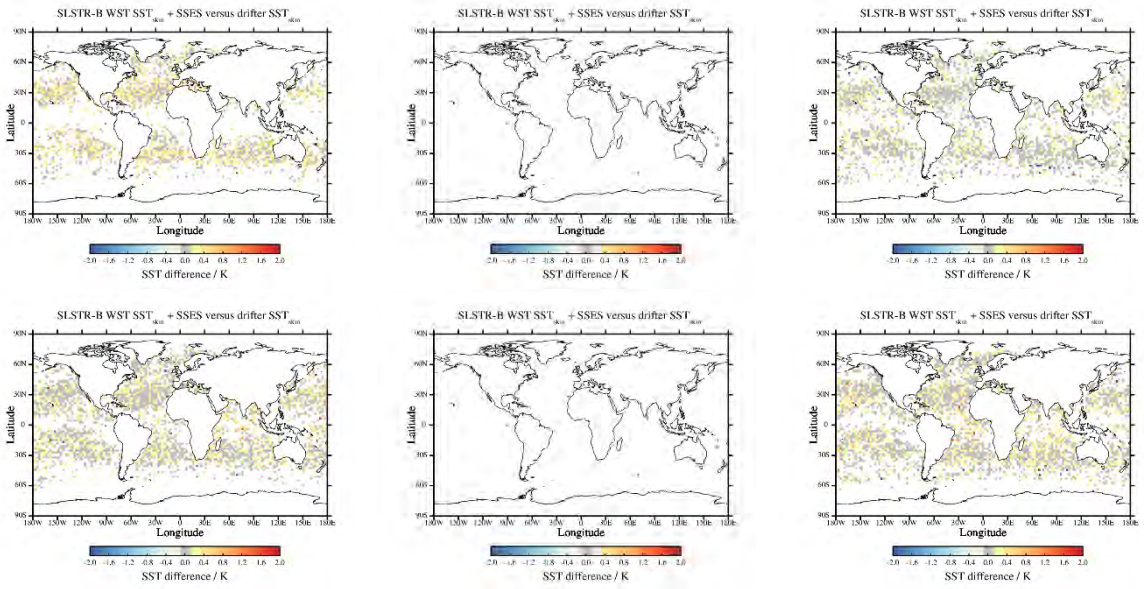

Figure 4-24: *Spatial distribution of the median discrepancy between SLSTR-B WST SST_{skin} and drifter SST_{skin}.*

4.4.2 Comparisons between SLSTR-B WST SSTs and Argo

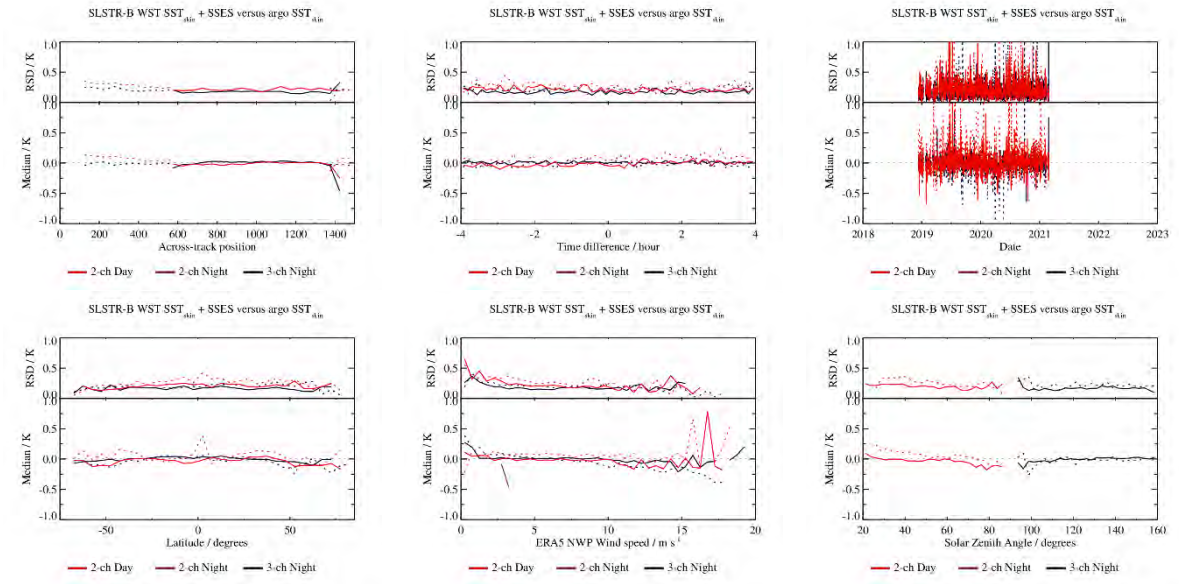

Figure 4-25: *Dependence of the median and robust standard deviation between SLSTR-B WST SST_{skin} and Argo SST_{skin}.*

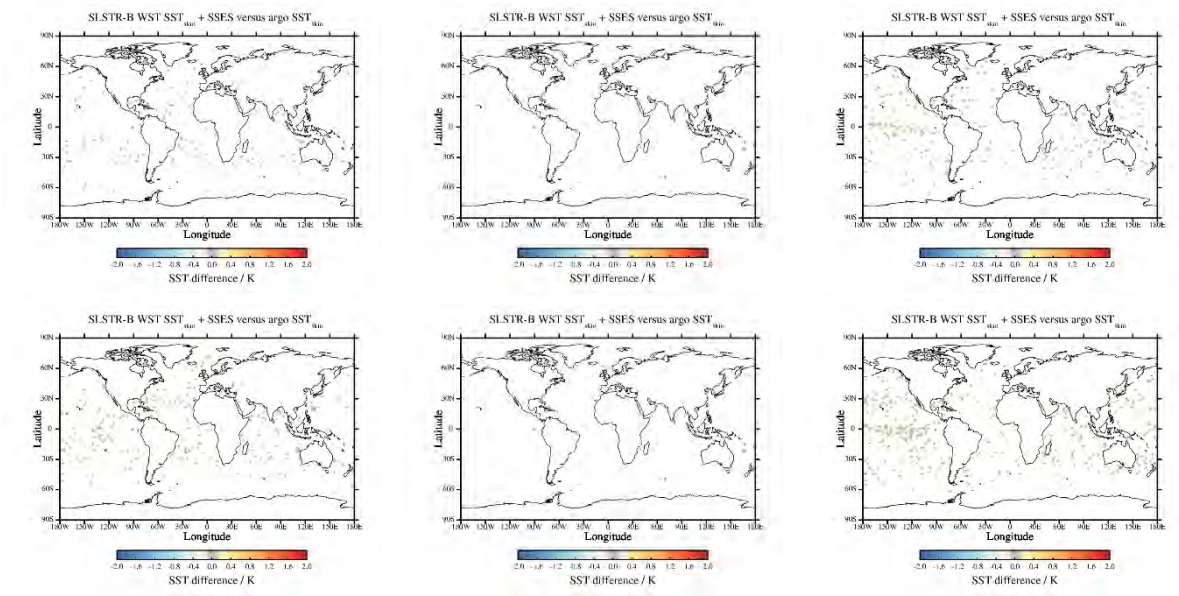

Figure 4-26: *Spatial distribution of the median discrepancy between SLSTR-B WST SST_{skin} and Argo SST_{skin}.*

4.4.3 Comparisons between SLSTR-B WST SSTs and moorings

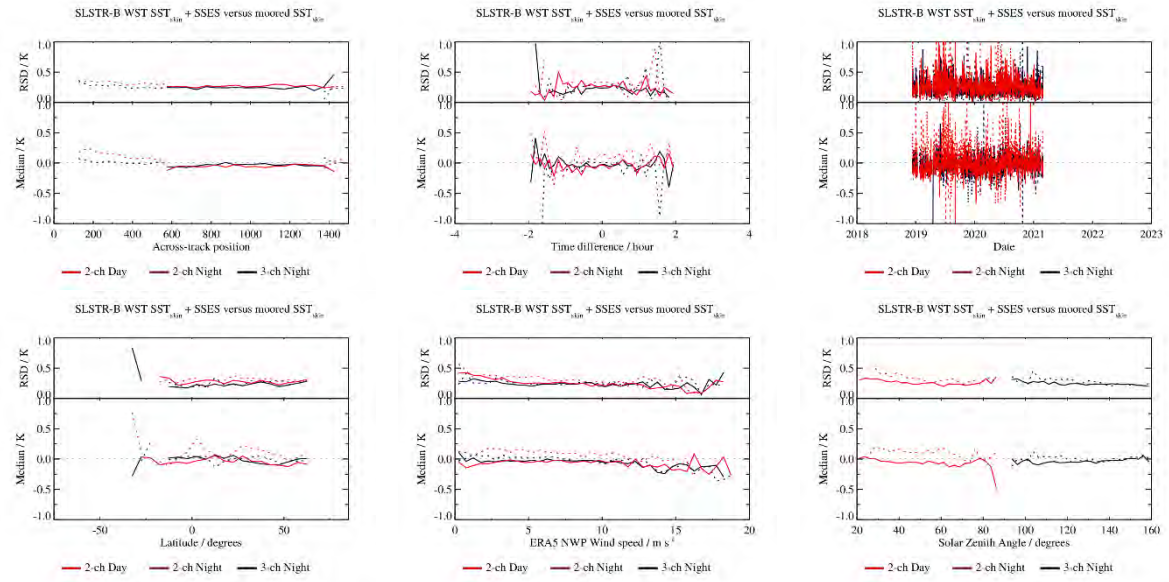

Figure 4-27: *Dependence of the median and robust standard deviation between SLSTR-B WST SST_{skin} and mooring SST_{skin}.*

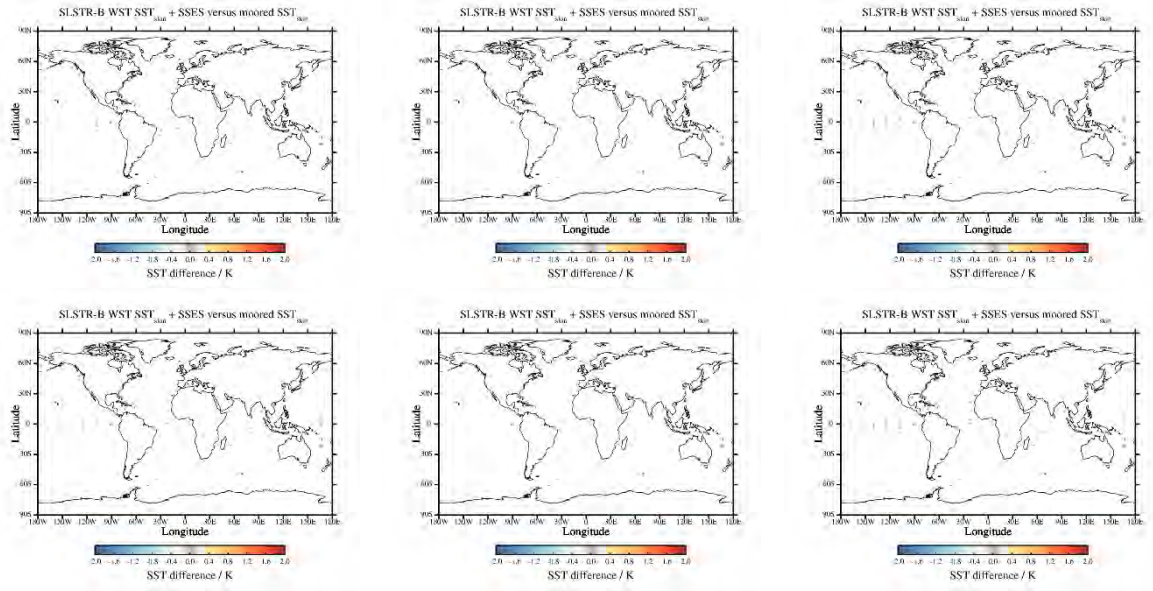

Figure 4-28: *Spatial distribution of the median discrepancy between SLSTR-B WST SST_{skin} and mooring SST_{skin}.*

4.4.4 Statistical analysis of SLSTR-B WST SST validation results

Reference	Retrieval	Number	Median (K)	RSD (K)
Drifters	*Day N2*	27213	+0.09	0.28
	Day D2	57920	+0.01	0.22
	Night N3	40297	+0.01	0.22
	Night D3	51187	+0.03	0.19
Mooring	*Day N2*	4670	+0.11	0.33
	Day D2	10643	-0.05	0.27
	Night N3	6803	+0.01	0.26
	Night D3	9092	-0.04	0.24
Argo	*Day N2*	2341	+0.07	0.28
	Day D2	4717	-0.01	0.22
	Night N3	3888	-0.01	0.20
	Night D3	5027	+0.01	0.17

Table 4-4: *Global validation statistics from comparing SLSTR-B Baseline Collection 3 WST SSTs to the available validation datasets.*

4.4.5 Discussion

The results for SLSTR-B WST SSTs are consistent with the results for the SLSTR-B WCT SSTs with small differences due to the use of atmospheric smoothing in the SL_2_WST product as also seen for SLSTR-A.

5 REFERENCES

[1] Coppo, P., Ricciarelli, B., Brandani, F., Delderfield, J., Ferlet, M., Mutlow, C., Munro, G., Nightingale, T., Smith, D., Bianchi, S.; et al. SLSTR: A high accuracy dual scan temperature radiometer for sea and land surface monitoring from space. J. Mod. Opt. 2010, 57, 1815–1830.

[2] Drinkwater, M.R.; Rebhan, H. Sentinel-3 Mission Requirements Document.Sentinel-3 Project Document, EOP-SMO/1151/MD-md; ESA, ESTEC: Noordwijk, The Netherlands, 2007.

[3] Donlon, C.; Sentinel-3 Mission Requirements Traceability Document. Sentinel-3 Project Document, EOP-SM/2184/CD-cd; ESA, ESTEC: Noordwijk, The Netherlands, 2011.

[4] Rebhan, H., Goryl, P., Donlon, C., Féménias, P., Bonekamp, H., Fournier-Sicre, V., Kwiatkowska, E., Montagner, F., Nogueira-Loddo, C., O'Carroll, A. Sentinel-3 Calibration and Validation Plan; Sentinel-3 Project Document, S3-PL-ESA-SY-0265; ESA, ESTEC: Noordwijk, The Netherlands, 2012.

[5] Embury, O.; Merchant, C.J.; Filipiak, M.J. A reprocessing for climate of sea surface temperature from the along-track scanning radiometers: Basis in radiative transfer. Remote Sensing of Environment 2012, 116, 32-46.

[6] Merchant, C.J., Harris, A.R., Maturi, E. & MacCallum, S. Probabilistic physically-based cloud screening of satellite infra-red imagery for operational sea surface temperature retrieval. Quarterly Journal of the Royal Meteorological Society, 131 (611), 2735-2755.

[7] Donlon, C.J., Minnett, P.J., Gentemann, C., Nightingale, T.J., Barton, I.J., Ward B., and Murray, M.J., 2002. Toward Improved Validation of Satellite Sea Surface Skin temperature Measurements for Climate Research, Journal of Climate, 15, 353-369

[8] Fairall, C., Bradley, E., Godfrey, J., Wick, G., Edson, J., and Young, G., 1996. Cool-skin and warm-layer effects on sea surface temperature, Journal of Geophysical Research, 101(C1), 1295-1308.

[9] Kantha, L.H., and Clayson, C.A., 1994. An improved mixed layer model for geophysical applications, Journal of Geophysical Research, 99, C12, 25235-25266.

[10] Embury, O., Merchant, C.J., Corlett, G.K., 2012. A reprocessing for climate of sea surface temperature from the along-track scanning radiometers: Initial validation, accounting for skin and diurnal variability effects. Remote Sensing of Environment, 116, 62–78.

[11] Horrocks, L.A., Candy, B., Nightingale, T., Saunders, R.W., O'Carroll, A.G., Harris, A.R., 2003. Parameterisations of the skin effect and implications for satellite-based measurement of sea-surface temperature, Journal of Geophysical Research, 108 (C3).

[12] Hersbach, H., Bell, B., Berrisford, P., Biavati, G., Horányi, A., Muñoz Sabater, J., Nicolas, J., Peubey, C., Radu, R., Rozum, I., Schepers, D., Simmons, A., Soci, C., Dee, D., Thépaut, J-N. (2018): ERA5 hourly data on single levels from 1979 to present. Copernicus Climate Change Service (C3S) Climate Data Store (CDS).

[13] Taberner, M., Shutler, J., Walker, P., Poulter, D., Piolle, J.-F., Donlon, C., and Guidetti, V., (2013) The ESA FELYX High Resolution Diagnostic Data Set System Design and Implementation. ISPRS – International Archives of the Photogrammetry, Remote Sensing and Spatial Information Sciences, XL-7/W2, 243–249.